

Nanofluidic Ion Transport through Reconstructed Layered Materials

Kalyan Raidongia and Jiaying Huang*

Department of Materials Science and Engineering, Northwestern University, Evanston, Illinois 60208, United States

S Supporting Information

ABSTRACT: Electrolytes confined in nanochannels with characteristic dimensions comparable to the Debye length show transport behaviors deviating from their bulk counterparts. Fabrication of nanofluidic devices typically relies on expensive lithography techniques or the use of sacrificial templates with sophisticated growth and processing steps. Here we demonstrate an alternative approach where unprecedentedly massive arrays of nanochannels are readily formed by restacking exfoliated sheets of layered materials, such as graphene oxide (GO). Nanochannels between GO sheets are successfully constructed as manifested by surface-charge-governed ion transport for electrolyte concentrations up to 50 mM. Nanofluidic devices based on reconstructed layer materials have distinct advantages such as low cost, facile fabrication, ease of scaling up to support high ionic currents, and flexibility. Given the rich chemical, physical, and mechanical properties of layered materials, they should offer many exciting new opportunities for studying and even manufacturing nanofluidic devices.

Fluids confined in nanoscale channels, with characteristic size typically on the order of 1–100 nm, could exhibit significantly different properties from their bulk counterparts.^{1,2} In particular, when the dimensions of the channels are close to the Debye screening length, the surface charge of the channels can drastically alter the ionic behaviors of the nanofluids. For example, when a bias is applied to an electrolyte solution, both cations and anions act as charge carriers, contributing to the overall ionic current. However, in nanofluidic channels, the surface charge of the channels will effectively repel the co-ions, allowing only the counterions to transport through.^{3,4} Moreover, to balance the surface charge, the counterions are concentrated inside the channels, thus enhancing the ionic conductivity.^{5,6} Potential applications of nanofluidics include electrical energy conversion,⁷ DNA manipulation and sequencing,^{8–10} and ionic concentration/separation devices.^{11,12} Since Debye screen length is inversely proportional to the square root of ionic concentration, the characteristic size of the channels has to be drastically reduced to allow nanofluidic transport at higher electrolyte concentrations. For example, channels with size on the order of 100 nm are required for salt concentration greater than 0.1 mM, which is below the resolution of conventional photolithography. In addition to expensive lithography techniques^{5,13,14} to fabrication nanofluidic channels, sub-100 nm cylindrical nanofluidic channels have been made using nanowires as sacrificial template.^{15–17} Arrays of sub-10 nm channels have been made from surfactant-templated

mesoporous silica thin films produced by a dip-coating process.¹⁸ Carbon nanotubes have been employed directly as nanofluidic channels, too.^{19,20} Two-dimensional (2D) channels with small height but much wider lateral dimensions have been realized by a two-step “etching and bonding” approach.^{21,22}

Here we report a novel approach to create nanofluidic devices based on reconstructed layered materials. When exfoliated single atomic/molecular sheets such as negatively charged graphene oxide (GO) are restacked together, they can regenerate a free-standing, paper-like layered structure²³ with tunable interlayer spacing comparable to their apparent thickness, typically of just few nanometers. Although the lateral size of the sheets can be very polydisperse, the restacked structure shall still readily produce numerous interconnected 2D nanofluidic channels. Nanofluidic channels fabricated by lithography and template-based methods usually have better defined geometries, but the reconstructed multilayer structures offer many unique features and distinct advantages: (1) The paper-like thin films are much easier to fabricate and can be modified without any lithography or sophisticated material growth and processing steps. It is particularly attractive that channels a few nanometers thick can now be made with ease, which are very challenging to fabricate otherwise. (2) The macroscopic dimensions of the paper makes it very convenient to address the nanofluidic channels, thus eliminating the need for microfluidic “contacts” that are usually required to interface the nanofluidic channels with external electrodes. (3) Papers of restacked sheets can be readily scaled up in terms of thickness and lateral dimensions, leading to unprecedentedly massive arrays of nanofluidic channels capable of generating much higher ionic flux and currents. (4) The surface charge and channel height can be potentially tuned by modifying the sheets before assembly, avoiding the challenges of chemically functionalizing the inner surface of nanochannels. (5) The reconstructed papers are flexible, making it possible to integrate nanofluidic devices with other flexible circuits. (6) The optoelectrical properties of the layered constituents can be potentially utilized to create new opportunities for controlling the nanofluids.

Regular GO sheets made from graphite powders are typically ~1 nm thick, but their lateral dimensions can readily extend to tens of micrometers.²⁴ These very different length scales make restacked GO paper a unique intermediate between fabricated nanofluidic devices and common porous material in terms of the fabrication/synthesis and structures of the channels/pores. Compared to common nanoporous materials such as zeolites, mesoporous silica, or Nafion,²⁵ for which the porosity control is

Received: August 17, 2012

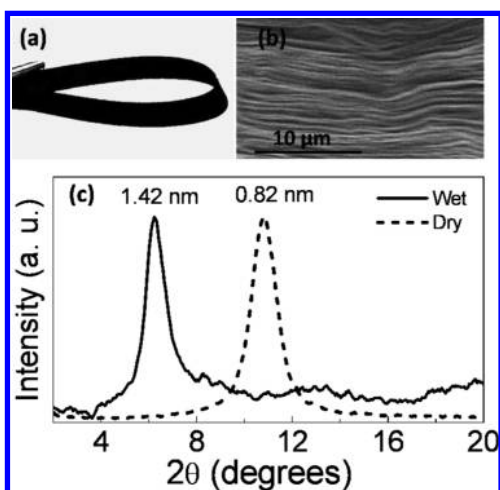


Figure 1. (a) A flexible GO strip with lamellar structure as shown in the cross-sectional SEM image in (b). (c) XRD patterns of air-dried and fully hydrated GO papers.

typically achieved by molecular design and assembly, GO and potentially other 2D materials offer much more straightforward ways to tune porosity by simply stacking the sheets. In this regard, restacked layered materials can be viewed as a new platform bridging the studies in nanofluidics and nanoporous materials.

In this work, we demonstrate the proof of concept of such flexible nanofluidic devices using GO paper. GO sheets are essentially graphene decorated by various oxygen-containing groups such as carboxylic acid, phenyl hydroxide, and epoxy groups.²⁴ Therefore, they are negatively charged when dispersed in water.²⁶ Although the lateral dimensions of GO can readily extend to tens of micrometers, its apparent thickness, determined by atomic force microscopy (AFM), is ~ 1 nm.²⁷ The soft GO sheets can restack to form a flexible paper-like film (Figure 1a) upon drying or filtration. Prior X-ray diffraction (XRD) studies found that the interlayer spacing in GO stacks is also ~ 1 nm, which is tunable by the degree of hydration²⁸ or intercalation of other guest molecules.²⁹ Here we show that the intersheet spacing can effectively function as nanofluidic channels for ionic transport.

GO was synthesized on the basis of a modified Hummers's method,³⁰ purified by a two-step washing route,³¹ and filtered to obtain a free-standing paper. AFM studies on multiple GO sheets confirm that their height is ~ 1 nm (Figure S1a). Fluorescence quenching microscopy (FQM)^{32,33} evaluation of GO sheets reveals that their lateral dimensions are around a few micrometers to tens of micrometers (Figure S1b). Due to their extremely high aspect ratio, the GO sheets should stack horizontally after vacuum filtration to create aligned 2D nanochannel arrays.²³ To fabricate a GO paper-based nanofluidic device, the paper was first cut by scissors into desirable shapes and sizes (Figure 1a). For the work described here, rectangular strips of dimensions ~ 12 mm \times 7 mm were used. Scanning electron microscopy (SEM) examination of the cross-section confirms the formation of well-stacked GO layers (Figure 1b). No large pores or large chunk of disordered flakes were observed. XRD patterns in Figure 1c show that the average interlayer spacing of an air-dried GO paper increases from ~ 0.82 nm to ~ 1.42 nm upon full hydration by soaking in water overnight. Next, the GO strip was immersed in a blend of polydimethylsiloxane (PDMS) prepolymer and curing agent.

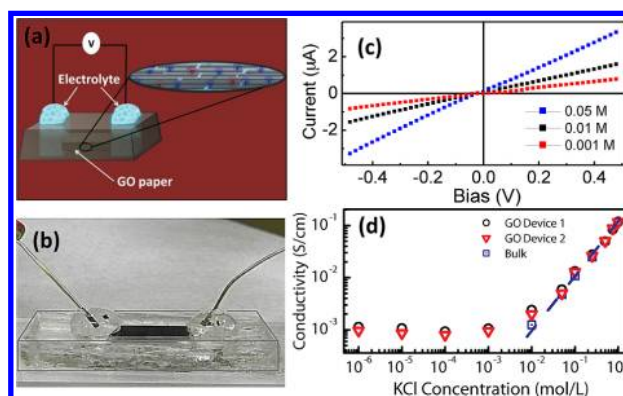


Figure 2. (a) Schematic illustration and (b) photograph showing GO paper-based nanofluidic device. (c) Representative I - V curves recorded at different KCl concentrations. (d) Ionic conductivity as a function of salt concentration measured through GO nanochannels. Results of two devices are presented here, showing good consistency. Conductivity of bulk solution is shown as a reference.

After curing, the strip was embedded in the PDMS elastomer. To complete the device, two reservoirs of about 0.3 mL in volume were carved out in the PDMS, exposing the two ends of the GO strip to electrolyte solution such as KCl (Figure 2a). Ag/AgCl electrodes were inserted into both the source and drain reservoirs to measure ionic current through the GO paper (see Figure 2b). All the measurements were done on a probe station equipped with a Keithley 2601A source meter inside a Faraday cage. The as-made devices were then soaked in deionized water for a few days to ensure hydration of the GO channels. Wetting of GO paper by water can be monitored by measuring ionic conductance through source and drain (Figure S2a). Initially, no detectable conductance was observed. Measurable ionic conductance was observed after about 5 h of exposure to water, which then increased gradually over time and reached steady state after another ~ 15 h. This should correspond to complete hydration and swelling of the GO paper embedded in the PDMS matrix. The time needed for electrolytes to generate stable conductance through the GO channels can be determined using the same method (Figure S2b). In the experiments shown below, the GO devices were first soaked in water for an additional few days to ensure complete hydration of the GO channels, and then in the electrolytes for at least 24 h to obtain the steady-state conductance at the corresponding salt concentrations.

Figure 2c shows a set of representative current–voltage (I - V) curves at various salt concentrations. Remarkably, the centimeter-long GO device yielded ionic currents in the microampere regime, which are orders of magnitude higher than those of previously fabricated nanofluidic channel arrays.^{18,21,34} The GO papers used in this work are typically tens of micrometers thick, and are made of tens of thousands of layers. Therefore, they contain unprecedentedly massive arrays of few-nanometer-thick nanofluidic channels. Note that the scaling of GO nanofluidic devices is not at all limited by the film thickness, since individual papers can be easily stacked or connected in parallel on demand to support even higher current. The ionic conductivity as a function of KCl concentration for two different GO nanofluidic devices, made from strips cut from the same paper, is shown in Figure 2d. Conductivity of bulk KCl solution, which is proportional to concentration, is also included for comparison. The ionic transport characteristics of the GO devices have two distinct

features. At high salt concentration, ionic transport through GO paper is similar to that of the bulk electrolyte solution. However, it begins to deviate from bulk behavior at ~ 0.05 M and gradually plateaus at lower concentrations, showing the characteristic surface-charge-governed ionic transport. At this concentration regime, conductivity becomes independent of the nominal ionic concentrations. The negatively charged GO sheets can attract the K^+ cations but repel the Cl^- anions, which leads to drastically higher than bulk, nearly constant cationic concentrations due to the small volume of the nanochannels. Therefore, the ionic conductivity at the plateau regime is also much higher than the bulk values. Since GO sheets are much smaller than the final GO paper, the 2D nanochannels between each pair of neighboring layers must interconnect to form a network to allow ionic conductance. Although defects such as microscopic voids or stacking faults could exist in the GO paper, nanofluidic ionic transport behaviors will still be observed, as long as the defects are not percolated along the direction of ionic current. The conductivity curves of GO paper devices shown in Figure 2d indicate successful construction of nanofluidic channel networks, as well as the absence of percolated leakage pathways.

The conductivity (λ) is calculated from the equation $\lambda = G/(lw)$, where G is the measured conductance (i.e., slope of the $I-V$ curve) and l , h , and w are the length, height, and width of the channels, respectively. Conductivity of bulk electrolyte solution was measured on a rectangular trough with known l , h , and w dimensions ($7\text{ mm} \times 2\text{ mm} \times 2\text{ mm}$), and the values were comparable to literature results. To calculate the ionic conductivity of GO channels, the effective combined height of the stacked nanochannels h needs to be determined first. The value of h is deduced to be $\sim 35\ \mu\text{m}$ from the conductance at high salt concentration regime (i.e., 1 M), where the nanochannels also show bulk-solution-like conductance. Next, λ of nanochannels at lower salt concentrations can be calculated accordingly. Figure 2d also shows that the ionic conductivity of different devices made from the same piece of GO paper is highly consistent.

The conductance of a nanochannel filled with electrolyte should include the contributions from both the bulk type of conductance and the double-layer determined conductance:^{35–37}

$$G_0 = 2\mu_K\sigma_s(w/l) + q(\mu_K + \mu_{Cl})C_B N_A w h_0 / l$$

Here the left term is the surface-charge-governed conductance, which dominates at low salt concentration (C_B). The right term is the bulk conductance, which dominates at high concentration. G_0 is the conductance of a single channel, which can be calculated by dividing the conductance of a GO paper device by n . μ_K and μ_{Cl} are mobilities of K^+ and Cl^- , respectively. N_A is Avogadro's number, and q is elementary charge. h_0 is the height of the nanochannels between neighboring GO sheets. XRD results in Figure 1c suggest that the average interlayer spacing in hydrated GO paper is $\sim 1.42\text{ nm}$. Since the thickness of graphene basal plane (i.e., extension of electronic clouds) is estimated to be 0.35 nm ,³⁸ the available space for electrolyte solution, i.e., the height of the nanofluidic channels h_0 , is 1.07 nm . If we assume the GO paper contains a stack of discrete parallel channels, the total number of channels n can be estimated to be $h/h_0 = 32\ 609$. Thus, σ_s can thus be determined to be 0.77 mC/m^2 . With the rich chemistry of GO, σ_s should be tunable by chemical functionalization of the sheets before assembling into multilayers to control the charge-governed

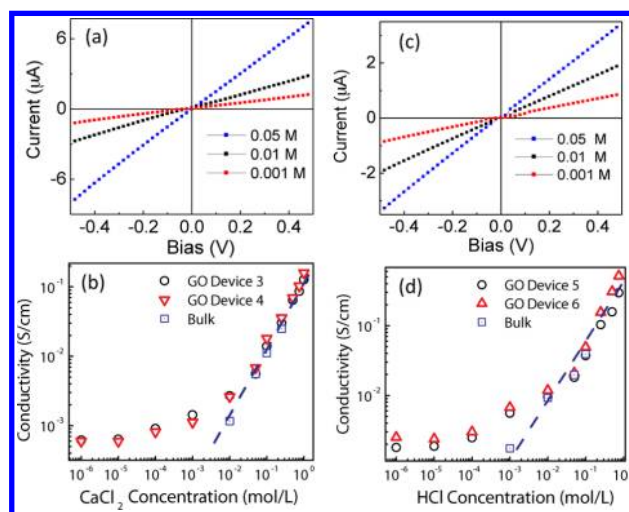


Figure 3. (a,c) Representative $I-V$ curves of the GO nanofluidic devices recorded at different CaCl_2 and HCl concentrations, respectively. (b,d) Concentration dependence of ionic conductivity through GO nanochannels for CaCl_2 and HCl , respectively. Results of two devices are given for both electrolytes, showing good consistency. Conductivity of bulk solution is also shown as a reference.

conductivity. For example, GO can be reduced and restacked to form graphene paper.²⁶ Unfortunately, in our preliminary studies, graphene paper-based devices did not show observable ionic conductance, likely due to their increased hydrophobicity, preventing water from entering the channels.

To test the versatility of GO paper-based devices, ion transport property was also studied for aqueous solutions of CaCl_2 and HCl (Figure 3). Representative $I-V$ curves at various CaCl_2 and HCl concentrations are shown in Figure 3a,c, respectively. Similar to KCl , both CaCl_2 and HCl yielded ionic currents in the microampere regime. The ionic conductivity as a function of electrolyte (CaCl_2 and HCl) concentrations is shown in Figure 3b,d, respectively. Here again at low concentrations (below 50 mM) a remarkable enhancement of ionic conductivity is observed that departs significantly from bulk behavior. At this concentration regime, conductivity is rather independent of electrolyte concentration, which is characteristic for surface-charge-governed ionic transport. As shown in Figure 3b,d, for both CaCl_2 and HCl , consistent results were obtained with different devices made with the same batch of GO paper.

The flexibility of GO paper made it feasible to create a flexible nanofluidics device. As a proof of concept, a rectangular GO paper strip of dimensions $\sim 27\text{ mm} \times 5\text{ mm}$ were used to make the device. The as-prepared GO device was highly flexible, as can be seen in Figure S3. Folding the GO strip embedded in PDMS in half, back and forth for 30 times, still yielded a working device. This suggests that GO-based nanofluidic channels are very robust and can be handled under high bending strain conditions. Moreover, the GO devices can be operated while being bent. Figure 4a,b shows the same GO nanofluidic device at curved and straight states, respectively. The bent device was fixed in a Petri dish (Figure 4a) during measurement so that the ratio of arch height (B) to arch length (L) was 0.25. The $I-V$ curves recorded at curved and straight states with 0.1 M KCl appear identical (Figure 4c). Figure 4d shows the ionic conductivity as a function of KCl concentration measured at 12 different concentrations ranging from pure water, 10^{-6} M , to 1 M. At each concentration, the

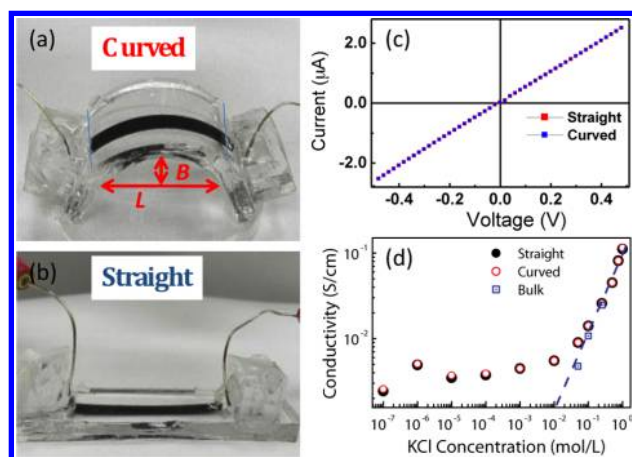


Figure 4. Photographs showing a GO nanofluidic device at (a) curved and (b) straight states, respectively. The bent device is fixed in a Petri dish so that the ratio of arch height to length $B/L = 0.25$. (c) Representative $I-V$ curves recorded at 0.1 M KCl concentration at both the straight and curved states. (d) Salt concentration-dependent ionic conductivity of the device measured at both the bent and straight states, showing that the device is not affected by bending. Conductivity of bulk solution is shown as a reference.

device was measured at both bent and straight states. The good overlap between the two set of data suggests that the GO device was not affected at all by bending.

In conclusion, nanofluidic ion transport through GO paper has been demonstrated. By assembling GO sheets into a multilayer, paper-like structure, numerous nanofluidic channels were formed with height of ~ 1 nm. Characteristic surface-charge-governed ion transport was observed for salt concentration up to ~ 50 mM. The ease of fabricating unprecedentedly massive arrays of nanochannels led to ionic currents in the microampere range with centimeter-long devices. The work here demonstrates the feasibility of creating large-scale, flexible nanofluidic devices through reconstructed layer materials. It should be possible to make GO electrically conductive through partially reduction to create gated nanofluidic devices. Given the rich selection of layered materials, their many possible ways for chemical functionalization, and their intrinsic optoelectrical properties, layered materials or their hybrids should offer many exciting new opportunities for studying and even manufacturing nanofluidic devices and materials.

■ ASSOCIATED CONTENT

● Supporting Information

AFM and FQM images of GO sheets, time-dependent ionic conductance during soaking of the GO device in water and 1 M KCl, and a photograph showing one fully bent GO nanofluidic device. This material is available free of charge via the Internet at <http://pubs.acs.org>.

■ AUTHOR INFORMATION

Corresponding Author

jiaxing-huang@northwestern.edu

Notes

The authors declare no competing financial interest.

■ ACKNOWLEDGMENTS

K.R. acknowledges the Indo-US Science & Technology Forum (IUSSTF) for a postdoctoral fellowship. J.H. acknowledges the Alfred P. Sloan Foundation for a Sloan Research Fellowship.

■ REFERENCES

- (1) Abgrall, P.; Nguyen, N.-T. *Nanofluidics*; Artech House: Boston, 2009.
- (2) van den Berg, A.; Craighead, H. G.; Yang, P. *Chem. Soc. Rev.* **2010**, *39*, 899.
- (3) Wei, C.; Bard, A. J.; Feldberg, S. W. *Anal. Chem.* **1997**, *69*, 4627.
- (4) Siwy, Z.; Gu, Y.; Spohr, H. A.; Baur, D.; Wolf-Reber, A.; Spohr, R.; Apel, P.; Korchev, Y. E. *Europhys. Lett.* **2002**, *60*, 349.
- (5) Stein, D.; Kruithof, M.; Dekker, C. *Phys. Rev. Lett.* **2004**, *93*, 035901.
- (6) Daiguji, H. *Chem. Soc. Rev.* **2010**, *39*, 901.
- (7) Daiguji, H.; Yang, P. D.; Szeri, A. J.; Majumdar, A. *Nano Lett.* **2004**, *4*, 2315.
- (8) Levy, S. L.; Craighead, H. G. *Chem. Soc. Rev.* **2010**, *39*, 1133.
- (9) Fan, R.; Karnik, R.; Yue, M.; Li, D. Y.; Majumdar, A.; Yang, P. D. *Nano Lett.* **2005**, *5*, 1633.
- (10) Han, J.; Craighead, H. G. *Science* **2000**, *288*, 1026.
- (11) Kim, S. J.; Song, Y. A.; Han, J. *Chem. Soc. Rev.* **2010**, *39*, 912.
- (12) Piruska, A.; Gong, M.; Sweedler, J. V.; Bohn, P. W. *Chem. Soc. Rev.* **2010**, *39*, 1060.
- (13) Cao, H.; Yu, Z.; Wang, J.; Tegenfeldt, J. O.; Austin, R. H.; Chen, E.; Wu, W.; Chou, S. Y. *Appl. Phys. Lett.* **2002**, *81*, 174.
- (14) Turner, S. W. *J. Vac. Sci. Technol., B* **1998**, *16*, 3835.
- (15) Fan, R.; Karnik, R.; Yue, M.; Li, D.; Majumdar, A.; Yang, P. *Nano Lett.* **2005**, *5*, 1633.
- (16) Fan, R.; Yue, M.; Karnik, R.; Majumdar, A.; Yang, P. *Phys. Rev. Lett.* **2005**, *95*, 086607.
- (17) Goldberger, J.; Fan, R.; Yang, P. *Acc. Chem. Res.* **2006**, *39*, 239.
- (18) Fan, R.; Huh, S.; Yan, R.; Arnold, J.; Yang, P. *Nat. Mater.* **2008**, *7*, 303.
- (19) Lee, C. Y.; Choi, W.; Han, J. H.; Strano, M. S. *Science* **2010**, *329*, 1320.
- (20) Liu, H.; He, J.; Tang, J.; Pang, P.; Cao, D.; Krstic, P.; Joseph, S.; Lindsay, S.; Nuckolls, C. *Science* **2010**, *327*, 64.
- (21) Duan, C.; Majumdar, A. *Nature Nanotechnol.* **2010**, *5*, 848.
- (22) Mao, P.; Han, J. *Lab Chip* **2005**, *5*, 837.
- (23) Dikin, D. A.; Stankovich, S.; Zimney, E. J.; Piner, R. D.; Dommett, G. H.; Evmenenko, G.; Nguyen, S. T.; Ruoff, R. S. *Nature* **2007**, *448*, 457.
- (24) Kim, J.; Cote, L. J.; Huang, J. *Acc. Chem. Res.* **2012**, *45*, 1356.
- (25) Mauritz, K. A.; Moore, R. B. *Chem. Rev.* **2004**, *104*, 4535.
- (26) Li, D.; Muller, M. B.; Gilje, S.; Kaner, R. B.; Wallace, G. G. *Nature Nanotechnol.* **2008**, *3*, 101.
- (27) Cote, L. J.; Kim, F.; Huang, J. *J. Am. Chem. Soc.* **2009**, *131*, 1043.
- (28) Lerf, A.; Buchsteiner, A.; Pieper, J.; Schöttl, S.; Dekany, I.; Szabo, T.; Boehm, H. P. *J. Phys. Chem. Solids* **2006**, *67*, 1106.
- (29) Stankovich, S.; Dikin, D. A.; Compton, O. C.; Dommett, G. H. B.; Ruoff, R. S.; Nguyen, S. T. *Chem. Mater.* **2010**, *22*, 4153.
- (30) Hummers, W. S.; Offeman, R. E. *J. Am. Chem. Soc.* **1958**, *80*, 1339.
- (31) Kim, F.; Luo, J.; Cruz-Silva, R.; Cote, L. J.; Sohn, K.; Huang, J. *Adv. Funct. Mater.* **2010**, *20*, 2867.
- (32) Kim, J.; Cote, L. J.; Kim, F.; Huang, J. X. *J. Am. Chem. Soc.* **2010**, *132*, 260.
- (33) Kim, J.; Kim, F.; Huang, J. X. *Mater. Today* **2010**, *13*, 28.
- (34) Wu, J.; Gerstandt, K.; Zhang, H.; Liu, J.; Hinds, B. J. *Nature Nanotechnol.* **2012**, *7*, 133.
- (35) Schoch, R. B.; Renaud, P. *Appl. Phys. Lett.* **2005**, *86*, 253111.
- (36) Guan, W.; Fan, R.; Reed, M. A. *Nat. Commun.* **2011**, *2*, 506.
- (37) Cheng, L. J.; Guo, L. J. *Nano Lett.* **2007**, *7*, 3165.
- (38) Nair, R. R.; Wu, H. A.; Jayaram, P. N.; Grigorieva, I. V.; Geim, A. K. *Science* **2012**, *335*, 442.